PNAS RESEARCH ARTICLE | PLANT BIOLOGY

A plant-specific module for homologous recombination repair

Xuanpeng Wang[a,b], Lili Wang[a,b], Yongchi Huang[a,b], Zhiping Deng[c], Cunliang Li[a,b], Jian Zhang[a,b], Mingxi Zheng[a,b], and Shunping Yan[a,b,1]

Edited by Yunde Zhao, University of California, San Diego, La Jolla, CA; received February 18, 2022; accepted March 11, 2022 by Editorial Board Member Julian I. Schroeder

Homologous recombination repair (HR) is an error-free DNA damage repair pathway to maintain genome stability and a basis of gene targeting using genome-editing tools. However, the mechanisms of HR in plants are still poorly understood. Through genetic screens for DNA damage response mutants (*DDRM*) in *Arabidopsis*, we find that a plant-specific ubiquitin E3 ligase DDRM1 is required for HR. DDRM1 contains an N-terminal BRCT (BRCA1 C-terminal) domain and a C-terminal RING (really interesting new gene) domain and is highly conserved in plants including mosses. The *ddrm1* mutant is defective in HR and thus is hypersensitive to DNA-damaging reagents. Biochemical studies reveal that DDRM1 interacts with and ubiquitinates the transcription factor SOG1, a plant-specific master regulator of DNA damage responses. Interestingly, DDRM1-mediated ubiquitination promotes the stability of SOG1. Consistently, genetic data support that SOG1 functions downstream of DDRM1. Our study reveals that DDRM1-SOG1 is a plant-specific module for HR and highlights the importance of ubiquitination in HR.

DNA damage response | homologous recombination repair | ubiquitination | SOG1

Significance

DNA damage causes genome instability and numerous diseases including cancers. Homologous recombination repair (HR) is an error-free pathway to repair DNA double-strand breaks, the most serious forms of DNA damage. However, the HR mechanisms in plants are still poorly understood. The transcription factor SOG1 is a master regulator of plant DNA damage responses. In this study, we find that a plant-specific ubiquitin E3 ligase DDRM1 ubiquitinates and stabilizes SOG1 to promote HR. Therefore, DDRM1- SOG1 is a plant-specific module for HR. DDRM1 is an evolutionarily ancient protein, which is identified in mosses, the first land plants, indicating that DNA damage response is an important mechanism for plant evolution from aquatic to land.

Various exogenous and endogenous factors can lead to DNA damage, which seriously threatens genome stability. Therefore, all organisms have evolved complex and sophisticated DNA damage responses (DDR) mechanisms in order to pass the correct genetic information to the next generations (1–3). In animals, defects in the DDR system can lead to many diseases, including various types of cancers (4). In contrast to animals, plants are sessile and thus cannot escape from environmental stresses, which usually cause the accumulation of reactive oxygen species (ROS), the toxic molecules to DNA (5, 6). In addition, plant photosynthesis is dependent on the sunlight, which contains the DNA-damaging ultraviolet light. It is believed that plants have both conserved and unique DDR mechanisms compared to other life kingdoms (7, 8). However, the DDR mechanisms in plants are still poorly understood (9, 10).

DNA double-strand breaks (DSBs) are the most serious forms of DNA damage. DSBs are mainly repaired by two pathways, nonhomologous end joining (NHEJ) and homologous recombination repair (HR). NHEJ is a highly efficient but error-prone mechanism functioning in all the cell-cycle phases, while HR is an error-free repair pathway restricted to the late S and G2 phases (11, 12). It is believed that NHEJ and HR compete to repair DSBs, and the underlying mechanism is extensively studied (13, 14). HR is also a basis of gene targeting using genome-editing tools such as CRISPR/CAS technology (15). However, the efficiency of gene targeting is very low in many organisms including flowering plants (16). There is a great need to improve HR efficiency. Therefore, studying the HR mechanism is of both scientific importance and potential implication.

The signaling pathway for HR was well-studied in mammals. As the DSB sensor, the Mre11-Rad50-Nbs1 (MRN) complex binds to DSB sites and recruits the protein kinase Ataxia-telangiectasia mutated (ATM), which phosphorylates itself and many downstream components including histone variant H2AX (17, 18). The phosphorylated H2AX (γH2AX) accumulates in DSB sites, generating the binding sites for mediator of DNA damage-checkpoint 1 (MDC1), which then is phosphorylated by ATM (19). The phosphorylated MDC1 recruits the ubiquitin E3 ligase RING finger protein 8 (RNF8), promoting the polyubiquitylation of histones 1, which is recognized by RNF168 (20–22). Subsequently, RNF168 mediates the polyubiquitination of H2A to recruit many ubiquitin-binding domain (UBD)-containing repair factors including receptor-associated protein 80 (RAP80), which further recruits another ubiquitin E3 ligase breast cancer susceptibility gene 1 (BRCA1). With the help of BRCA1, the recombinase RAD51 and its paralogs are recruited to the DSBs, leading to DSB repair through HR (23–26). Plants encode the orthologs of ATM, H2AX, BRCA1, and RAD51 but lack the orthologs of MDC1, RNF8, RNF168, and RAP80. Therefore, it remains elusive how plants repair DSBs through HR.

Author affiliations: [a]Hubei Hongshan Laboratory, Wuhan, 430070, China; [b]College of Life Science and Technology, Huazhong Agricultural University, Wuhan, 430070, China; and [c]State Key Laboratory for Managing Biotic and Chemical Threats to the Quality and Safety of Agro-products, Institute of Virology and Biotechnology, Zhejiang Academy of Agricultural Sciences, Hangzhou, 310021, China

Author contributions: X.W. and S.Y. designed the experiments; X.W., L.W., Y.H., Z.D., C.L., J.Z., and M.Z. carried out the experiments; and X.W., L.W., and S.Y. wrote the manuscript. All authors discussed the results and commented on the manuscript.

The authors declare no competing interest.

This article is a PNAS Direct Submission. Y.Z. is a guest editor invited by the Editorial Board.

[1]To whom correspondence may be addressed. Email: spyan@mail.hzau.edu.cn.

This article contains supporting information online at http://www.pnas.org/lookup/suppl/doi:10.1073/pnas.2202970119/-/DCSupplemental.

Published April 11, 2022.

SUPPRESSOR OF GAMMA RESPONSE 1 (SOG1) is a plant-specific NAC (NAM, ATAF1/2, and CUC2) transcription factor and was proposed to be the functional counterpart of p53, a master DDR regulator in mammals (27, 28). Genome-wide studies in *Arabidopsis* revealed that SOG1 can bind to the promoters of numerous genes involved in cell-cycle regulation, cell death, and HR (29). The functions of SOG1 are regulated through phosphorylation mediated by ATM, ATM- and Rad3-related (ATR), and casein kinase 2 (CK2) (30, 31). It remains to be explored whether other posttranslational modifications such as ubiquitination can regulate SOG1.

In this study, we performed a genetic screen for DNA damage response mutants (*DDRM*) in *Arabidopsis*. We found that the *ddrm1* mutant was hypersensitive to DSB-inducing reagents. DDRM1 is a plant-specific protein with an N-terminal BRCT (BRCA1 C-terminal) domain and a C-terminal RING (really interesting new gene) domain, both of which are essential for the function of DDRM1. DDRM1 localizes in the nucleus, where it directly interacts with, ubiquitinates, and stabilizes SOG1. We further showed that DDRM1 is required for HR. Our study uncovers a plant-specific HR regulator and highlights the importance of ubiquitination in HR, providing significant insights into plant DDR.

Results

DDRM1 Is Required for DSB Repair. The anticancer drug camptothecin (CPT) is an inhibitor of Topoisomerase I. It forms a tight complex with Topoisomerase I and DNA and prevents DNA religation, leading to formation of single-strand breaks (SSBs), which are converted to DSBs during DNA replication (32). CPT can also induce DSBs and inhibit root growth in *Arabidopsis* (33). To identify regulators of plant DDR, we performed a genetic screen for *DDRM* by examining the *Arabidopsis* root growth on CPT-containing medium. The plants with shorter or longer roots than wild-type (WT) were considered as *ddrm*s. Previous studies revealed that ATM is a central regulator of DDR (34). Compared with WT, the primary roots of the *atm-2* mutant were indistinguishable on the control medium but were much shorter on the medium containing 20 nM CPT (Fig. 1 and *SI Appendix*, Fig. S1). Therefore, we used the *atm-2* mutant as a positive control in the genetic screen. To identify potential transcription factors involved in DDR, we screened the TRANSPLANTA collection, which contains 1,636 independent homozygous lines with transcription factors under the control of a β-estradiol–inducible promoter (35). In the primary screening, 12 lines were found to show altered response to CPT compared with WT. Six lines were confirmed through rescreening. Here, we reported on one of the lines named *ddrm1-1*. Similar to *atm-2*, the *ddrm1-1* mutant was hypersensitive to CPT (Fig. 1 *A* and *B*). In the *ddrm1-1* mutant (TPT_3.57230.1A), the transcription factor AGL16 (AT3G57230) was conditionally overexpressed. However, the *ddrm1-1* mutant displayed shorter roots both in the presence or absence of β-estradiol on the CPT-containing medium (Fig. 1 and *SI Appendix*, Fig. S1), suggesting that it was not due to overexpression of AGL16 but due to T-DNA inserting into another gene. To determine the T-DNA insertion site in *ddrm1-1*, we performed high-efficiency thermal asymmetric interlaced PCR (hiTAIL-PCR) (36) and found that it was inserted into the first exon of *STUBL2* (SUMO-targeted ubiquitin ligase 2, AT1G67180, *SI Appendix*, Fig. S1*C*). Genotyping and reverse transcription–PCR (RT-PCR) analysis revealed that *ddrm1-1* was a knockout mutant (*SI Appendix*, Fig. S1 *D* and *E*).

STUBL2 was found to be a SUMO-interacting protein in a large-scale yeast two-hybrid screens (37). However, its biological function of STUBL2 is still unknown. To confirm *STUBL2* was the *DDRM1* gene, we crossed *ddrm1-1* with *ddrm1-2*, which contains a T-DNA insertion in the fourth intron of *STUBL2* and lacks detectable transcript (*SI Appendix*, Fig. S1 *C–E*). All F1 seedlings were hypersensitive to CPT (Fig. 1 *C* and *D*), indicating that the *ddrm1-2* mutant was allelic to *ddrm1-1*. In addition, when the coding sequence (CDS) of *STUBL2* driven by the 35S promoter was introduced into *ddrm1-1* or *ddrm1-2*, the resulting transgenic lines (*35S:DDRM1*) showed the same phenotypes as WT, suggesting that *STUBL2* can fully complement these *ddrm1* mutants (Fig. 1 *E* and *F* and *SI Appendix*, Fig. S1 *F* and *G*).

To further investigate the role of DDRM1 in DDR, we tested the sensitivity of *ddrm1-2* to other DNA-damaging reagents. Hydroxyurea (HU) is an inhibitor of ribonucleotide reductase and can induce replication stress. Bleomycin (BLM) and methyl methanesulfonate (MMS) are DSB-inducing reagents (38, 39). Compared with WT, *ddrm1-2* was significantly more sensitive to MMS and BLM, but not to HU (Fig. 1 *G* and *H*), indicating that DDRM1 was specifically involved in the DSB repair pathway.

DDRM1 Is a Plant-Specific Nuclear Protein. According to TAIR (https://www.arabidopsis.org), *DDRM1* has 7 splice variants. The representative variant *AT1G67180.1* was used for further analysis in this study. DDRM1 encodes a protein with 453 amino acid residues (aa). Conserved Domain Search (https://www.ncbi.nlm.nih.gov/Structure/cdd/wrpsb.cgi) revealed that DDRM1 contains a BRCT domain (4-76 aa) at N terminus and a RING domain (299-345 aa) at C terminus (*SI Appendix*, Fig. S2). BLAST (https://blast.ncbi.nlm.nih.gov/Blast.cgi) analysis indicated that DDRM1 is conserved in plants including mosses, the first land plants, but lacks orthologs in other life kingdoms, suggesting that DDRM1 is a plant-specific protein (Fig. 2*A*). The sequence alignment of representative DDRM1 orthologs using DNAMAN 7 revealed that the BRCT and RING domains are highly conserved, while the middle regions are not conserved (*SI Appendix*, Fig. S2).

To investigate the subcellular localization of DDRM1, GFP-DDRM1 driven by 35S promoter (35S:GFP-DDRM1) was transiently expressed in *Nicotiana* (*N.*) *benthamiana*. We found that GFP-DDRM1 localizes in the nucleus (Fig. 2*B*). We also generated the transgenic *Arabidopsis* lines expressing GFP-DDRM1. Consistently, the GFP fluorescence signal was detected in the nuclei of root meristem cells (Fig. 2*C*). To determine the expression patterns of *DDRM1*, we generated the transgenic *Arabidopsis* lines expressing YFP-GUS fusion protein driven by the *DDRM1* promoter (1,500 bp fragment upstream of the start codon). The 7-d-old transgenic seedlings were subjected to GUS staining. As shown in Fig. 2*D*, the GUS signal was mainly detected in the shoot and root apices, suggesting that *DDRM1* is highly expressed in the meristem.

Both RING and BRCT Domains Are Essential for the Function of DDRM1. To investigate the importance of RING and BRCT domain for the function of DDRM1, we generated two mutant forms of DDRM1. In DDRM1m1 (C341S/C344S), the conserved Cys341 and Cys344 of RING domain were mutated to Ser. In DDRM1m2 (W66A/C70A), the conserved Trp66 and Cys70 of BRCT domain were mutated to Ala. When DDRM1m1 or DDRM1m2 driven by 35S promoter were

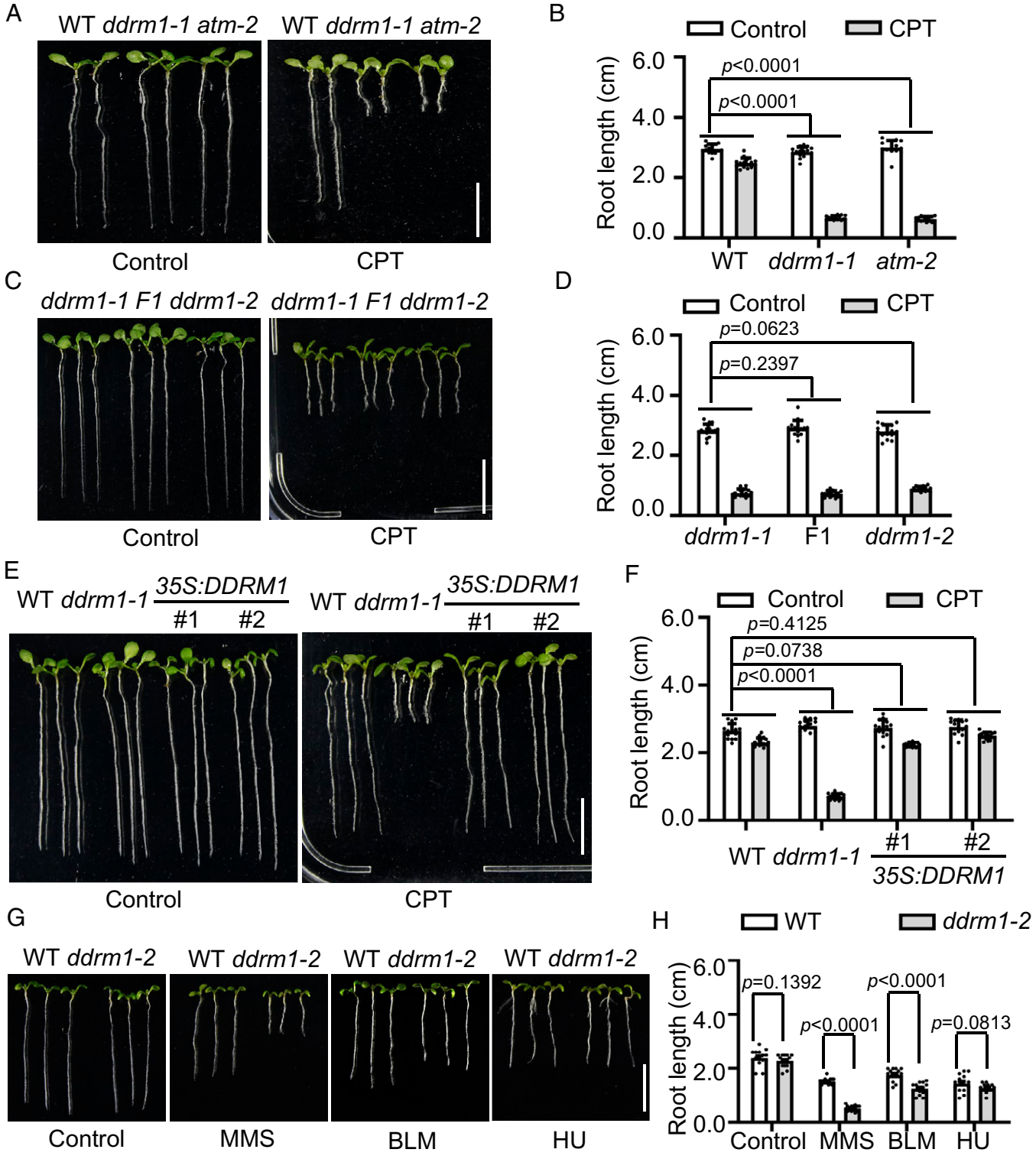

Fig. 1. The *ddrm1* mutant is specifically hypersensitive to DSB-inducing reagents. (*A*, *B*) The *ddrm1-1* mutant is hypersensitive to camptothecin (CPT). The *atm-2* mutant was used as a positive control. (*C*, *D*) The *ddrm1-1* mutant is allelic to the *ddrm1-2* mutant. F1, the F1 seedlings derived from the cross between *ddrm1-1* and *ddrm1-2*. (*E*, *F*) Overexpressing *DDRM1* rescues *ddrm1-1*. The CDS of *DDRM1* driven by the *35S* promoter was transformed into *ddrm1-1*. Two independent transgenic lines were shown. (*G*, *H*) The *ddrm1-2* mutant is hypersensitive to methyl methanesulfonate (MMS) and bleomycin (BLM), but not hydroxyurea (HU). The seedlings were grown vertically on the control medium or the medium containing 20 nM CPT, 75 μg/mL MMS, 5 μM BLM, or 1 mM HU for 8 d. The photos (*A*, *C*, *E*, *G*) and root length (*B*, *D*, *F*, *H*) of plants were shown. (Scale bars: 1 cm.) The root length was represented as means ± SD (n = 15). The statistical significance was determined using two-way ANOVA analysis.

introduced into *ddrm1-2*, the resulting transgenic lines were still hypersensitive to CPT (Fig. 3 *A*–*D*), indicating that both RING and BRCT domains are essential for the function of DDRM1.

DDRM1 Interacts with SOG1. Given that both BRCT and RING domains function as protein-interacting domain (40, 41), we hypothesized that DDRM1 functions by interacting with other proteins involved in DDR. It was shown that the

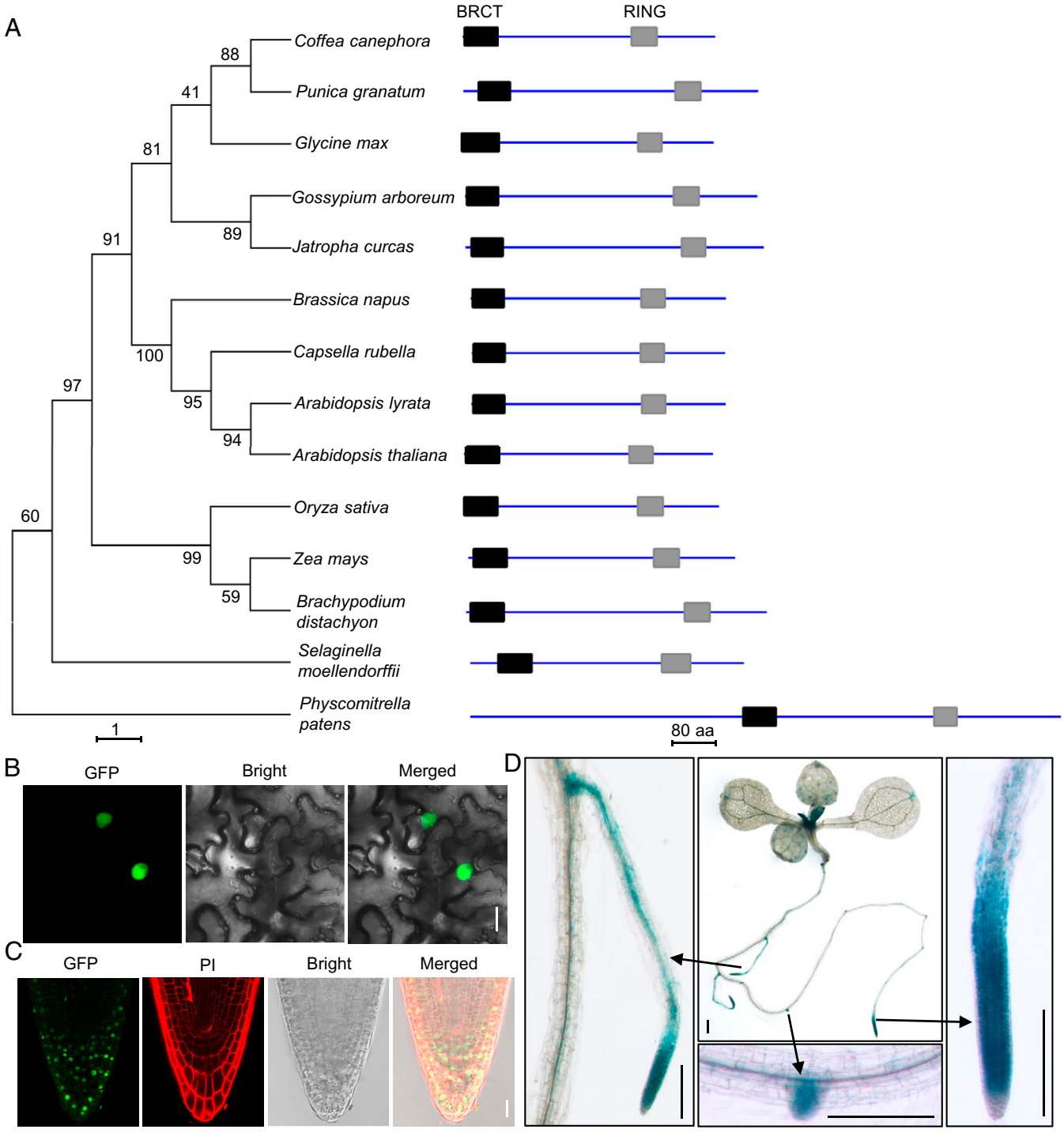

Fig. 2. DDRM1 localizes in the nucleus and is highly expressed in the meristem. (*A*) The phylogenetic relationship of DDRM1 and its orthologs from other plant species. The phylogenetic tree was constructed by the neighbor-joining method in MEGA-X. The BRCT domain and the RING domain were indicated by the black squares and gray squares, respectively. The amino acid sequences were retrieved from NCBI: *Coffea canephora* (CDP02383.1), *Punica granatum* (PKI75592.1), *Glycine max* (XP_014627684.1), *Gossypium arboretum* (XP_017616848.1), *Jatropha curcas* (XP_012088139.1), *Brassica napus* (CDY12624.1), *Capsella rubella* (XP_006302233.1), *Arabidopsis lyrate* (XP_002887108.1), *Arabidopsis thaliana* (Q9ZW89), *Oryza sativa* (XP_015649987.1), *Zea mays* (AQK52284.1), *Brachypodium distachyon* (XP_003574477.1), *Selaginella moellendorffii* (XP_002975153.1), and *Physcomitrella patens* (PNR36147.1). (*B*, *C*) The subcellular localization of DDRM1. The vector containing 35S:GFP-DDRM1 was transiently expressed in *N. benthamiana* leaves (*B*) or stably expressed in *Arabidopsis* (*C*). The roots of transgenic seedlings were stained with propidium iodide (PI) to show cell walls. The pictures were captured using confocal microscopy. (Scale bar: 20 μm.) (*D*) Histochemical staining of transgenic *Arabidopsis* expressing YFP-GUS driven the *DDRM1* promoter. (Scale bar: 0.2 mm.).

plant-specific transcription factor SOG1 is a master regulator of DDR (28). Therefore, we tested the interaction between DDRM1 and SOG1 using the split luciferase assays in *N. benthamiana* (42). DDRM1 was fused with the C-terminal half of luciferase (cLUC), and SOG1 was fused with the N-terminal half of luciferase (nLUC). An interaction between two proteins brings the two halves of the luciferase together, leading to enzymatic activity and production of luminescence, which can be detected by a hypersensitive CCD camera. As shown in Fig. 4*A*, the luminescence signal could be detected only when cLUC-DDRM1 and SOG1-nLUC were coexpressed, indicating that DDRM1 interacts with SOG1 in vivo. To confirm the

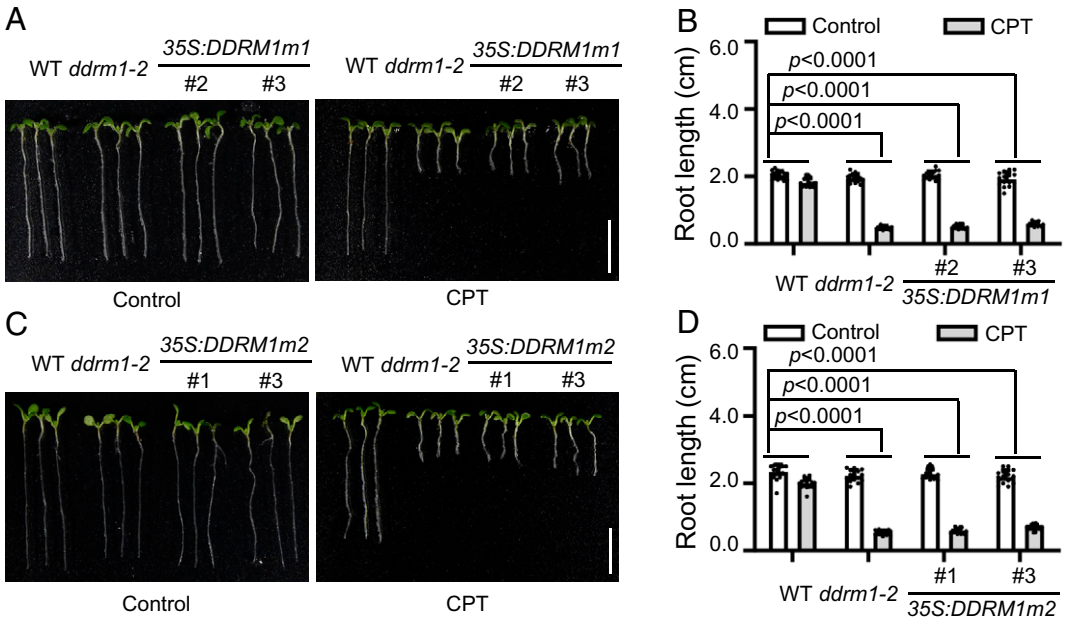

Fig. 3. Both RING and BRCT domains are required for the function of DDRM1. The DDRM1m1 (C341S/C344S) and DDRM1m2 (W66A/C70A) driven by the *35S* promoter were transformed into *ddrm1-2*. Two independent transgenic lines were grown vertically on the control medium or the medium containing 20 nM CPT for 8 d. The photos (*A*, *C*) and root length (*B*, *D*) of plants were shown. (Scale bars: 1 cm.) The root length was represented as means ± SD (n = 15). The statistical significance was determined using two-way ANOVA analysis.

interaction, we performed bimolecular fluorescence complementation (BiFC) and coimmunoprecipitation (CoIP) assays. In the BiFC assays, DDRM1 was fused to the N-terminal YFP (nYFP), and SOG1 was fused to the C-terminal YFP (cYFP). A strong nucleus-localized YFP fluorescence could be detected when SOG1-cYFP was coexpressed with DDRM1-nYFP in *N. benthamiana*. However, there was no YFP fluorescence when SOG1-cYFP was coexpressed with the GUS-nYFP control (Fig. 4*B*). In the CoIP assays, we used DDRM1m1 instead of DDRM1 because we found that the protein level of DDRM1 was much lower than DDRM1m1. The DDRM1m1-3xFLAG fusion protein was coexpressed with SOG1-GFP or GFP in *N. benthamiana*. The proteins were immunoprecipitated using GFP-Trap and were subjected to Western blotting analysis. Consistently, the DDRM1m1-3xFLAG protein could be coimmunoprecipitated by SOG1-GFP, but not the GFP control (Fig. 4*C*), suggesting that the mutations in RING domain does not affect its interaction with SOG1. To further examine whether DDRM1 directly interacts with SOG1, we performed in vitro pull-down assays using the purified maltose-binding protein-tagged SOG1 (MBP-SOG1) and glutathione S-transferase (GST)-tagged DDRM1 (GST-DDRM1) or GST. As shown in Fig. 4*D*, GST-DDRM1, but not GST, could pull down MBP-SOG1, indicating that DDRM1 directly interacts with SOG1. Taken together, these results indicated that DDRM1 can interact with SOG1 in vitro and in vivo.

DDRM1 Ubiquitinates SOG1. Many proteins containing RING domain function as ubiquitin E3 ligases (41). Since DDRM1 interacts with SOG1, we hypothesized that DDRM1 may further ubiquitinate SOG1. To test this hypothesis, we first examined whether SOG1 can be ubiquitinated in vivo. The ubiquitin (UBQ) tagged with 2xFLAG (2xFLAG-UBQ) and the 2xHA-tagged SOG1 (SOG1-2xHA) were coexpressed in *Arabidopsis* protoplasts. The proteins immunoprecipitated by anti-FLAG magnetic beads were subjected to Western blotting analysis using anti-HA antibody. Compared with the input sample, a major band ∼10 kDa larger than unmodified SOG1-2xHA was detected in the immunoprecipitation sample, suggesting that SOG1 is mainly monoubiquitinated in plants (Fig. 5*A*). Some weak bands with higher molecular weight were also observed, indicating that SOG1 may also be polyubiquitinated or monoubiquitinated at multiple sites.

To further investigate whether DDRM1 can ubiquitinate SOG1, we carried out in vitro ubiquitination assays using a reconstituted ubiquitination cascade system in *Escherichia coli* (43). E1 (AtUBA1), E2 (AtUBC8), UBQ10, MBP-SOG1-2xHA, DDRM1-Myc, or DDRM1m1-Myc were coexpressed in *E. coli* and the cell lysates were subjected to Western blotting analysis. As shown in Fig. 5*C*, the ubiquitination of SOG1 was detectable when the DDRM1 was coexpressed.

To identify the DDRM1-mediated ubiquitination sites of SOG1, we first tried to narrow down the ubiquitination regions by performing in vitro ubiquitination assays using SOG1 fragments (*SI Appendix*, Fig. S3*A*). We found that all SOG1 fragments could still be ubiquitinated by DDRM1 (*SI Appendix*, Fig. S3*B*), suggesting there are multiple ubiquitination sites in SOG1. Next, we purified MBP-SOG1-2xHA in the ubiquitination assays and subjected it to mass spectrometry (MS) analysis, which revealed that 23 Lys residues were ubiquitinated (Fig. 5*D*). Among them, K109, K246, K223, and K403 were on the top list (Fig. 5*D*). To confirm these ubiquitination sites, we performed in vitro ubiquitination assays using a SOG1 mutant with these four Lys residues replaced by Arg, named SOG1(4KR). The ubiquitination level of SOG1(4KR) were dramatically reduced, but not completely abolished (Fig. 5*E*). These results suggested that K109, K246, K223, and K403 were the main ubiquitination sites of SOG1 mediated by DDRM1.

DDRM1 Stabilizes SOG1. Given that DDRM1 ubiquitinates SOG1, we hypothesized that DDRM1 regulates the stability of SOG1. To test whether SOG1 is degraded through the 26S proteasome, we performed a cell-free degradation assay using

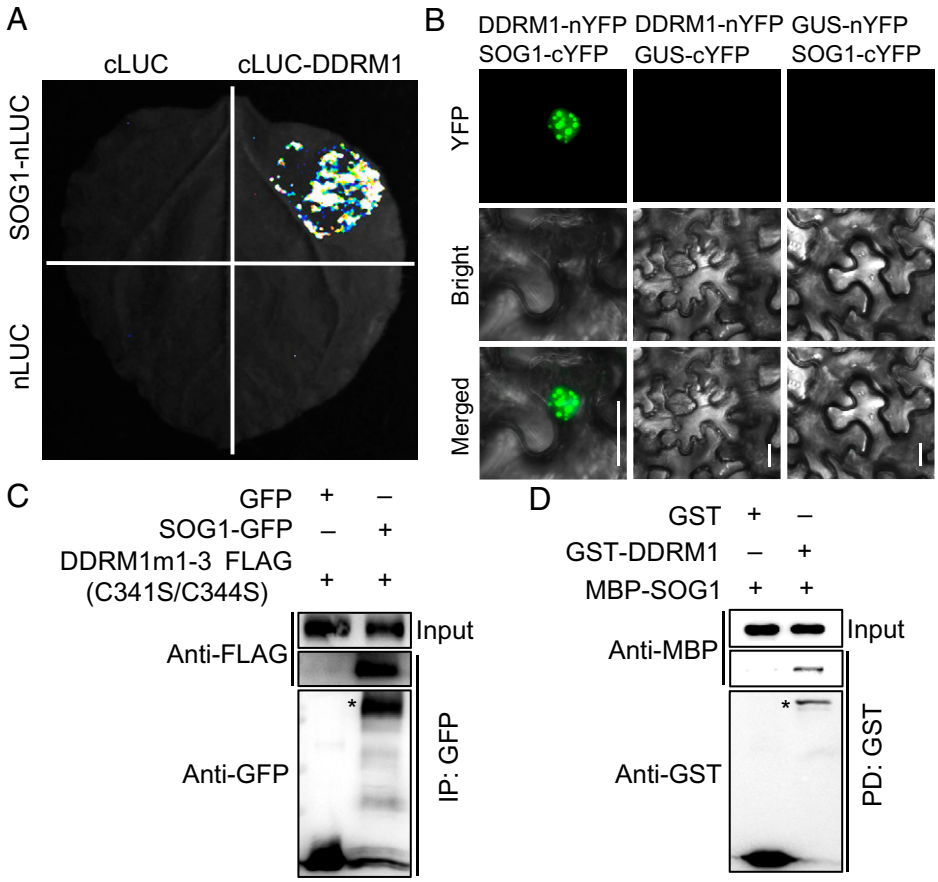

Fig. 4. DDRM1 directly interacts with SOG1. (*A*) Split luciferase assays. DDRM1 and SOG1 were fused to the C- and N-terminal half of luciferase (cLUC or nLUC), respectively, and were transiently expressed in *N. benthamiana.* The luminesce detected by a CCD camera indicates interaction. (*B*) BiFC assays. SOG1 and DDRM1 were fused to the C- and N-terminal half of YFP (cYFP or nYFP), respectively, and were transiently expressed in *N. benthamiana.* The YFP fluorescence detected by confocal microscopy indicates interaction. (Scale bars: 20 μm). (*C*) CoIP assays. DDRM1m1 fused with three tandem FLAG tag (DDRM1m1-3xFLAG) was transiently coexpressed with SOG1-GFP or GFP in *N. benthamiana*. Immunoprecipitation was performed using GFP-Trap beads and bound proteins were subjected to Western blotting using anti-FLAG or anti-GFP antibodies. (*D*) In vitro pull-down assays. The recombinant GST or GST-DDRM1 proteins were coupled to glutathione beads and incubated with the recombinant MBP-SOG1 protein. Bound proteins were detected by Western blotting using anti-GST or anti-MBP antibodies.

the recombinant MBP-SOG1 protein. MBP-SOG1 were incubated with the total protein extract of *Arabidopsis* at room temperature for different time. Western blotting analysis revealed that the levels of MBP-SOG1 was gradually decreased over time and the degradation was largely blocked by MG132, a 26S proteasome inhibitor (Fig. 6*A*).

To investigate whether DDRM1 regulates the stability of SOG1, we examined the protein levels of SOG1-2xHA in the presence or absence of DDRM1 in plants. To this end, SOG1-2xHA was coexpressed with DDRM1-GFP or GFP in *N. benthamiana*. The CFP-HA in the same vector of SOG1-2xHA was used as an internal control. Compared with GFP, DDRM1-GFP dramatically enhanced the protein level of SOG1-2xHA (Fig. 6*B*), indicating that DDRM1 stabilizes SOG1. Interestingly, DDRM1 could not stabilize SOG1(4KR) (*SI Appendix*, Fig. S4), highlighting the importance of these ubiquitination sites. To further confirm our conclusion, we generated transgenic lines expressing DDRM1-GFP driven by the dexamethasone (DEX)-inducible promoter (*pGVG:DDRM1-GFP*) using *35S:SOG1-2xHA/ddrm1-2* as background. After DEX treatment, the protein levels of DDRM1-GFP and SOG1-2xHA were increased correlatedly (Fig. 6*C*), suggesting that DDRM1 is sufficient to stabilize SOG1.

Next, we tested whether DDRM1 is required for SOG1 stability by performing in vivo degradation assay. To exclude the effect of transgene expression level, the transgenic line expressing *35S:SOG1-2xHA* in WT background was crossed with *ddrm1-2* to generate *35S:SOG1-2xHA/ddrm1-2*. Both lines were treated with chlorhexidine (CHX) to inhibit protein synthesis and allow protein degradation. As shown in Fig. 6*D*, SOG1-2xHA was more easily degraded in the *ddrm1-2* than in WT. Taken together, we concluded that DDRM1 is necessary and sufficient to stabilize SOG1.

SOG1 Functions Downstream of DDRM1. SOG1 is a master regulator of DDR. In addition to DNA repair, it also regulates cell-cycle progression and cell death. Previous studies have shown that the *sog1* mutant is more resistance to DSBs than WT (27). To determine the genetic relationship between DDRM1 and SOG1, we sought to test the phenotypes of the *ddrm1 sog1* double mutant in response to CPT. The *sog1-102* mutant (GABI_143A02) contained a T-DNA insertion in the first intron of *SOG1* and was a knockout mutant as revealed by the RT-PCR analysis (*SI Appendix*, Fig. S5). We crossed *ddrm1-2* with *sog1-102* to generate the *ddrm1-2 sog1-102* double mutant. Although the root length of *sog1-102* was similar to that WT, the *ddrm1-2 sog1-102* double mutant was significantly longer than *ddrm1-2* (Fig. 7 *A* and *B*). In consistence, we also found that overexpressing of SOG1 in *ddrm1-2* could enhanced the sensitivity of *ddrm1-2* to CPT (Fig. 7 *C* and *D*). These genetic data suggested that SOG1 functions downstream of DDRM1.

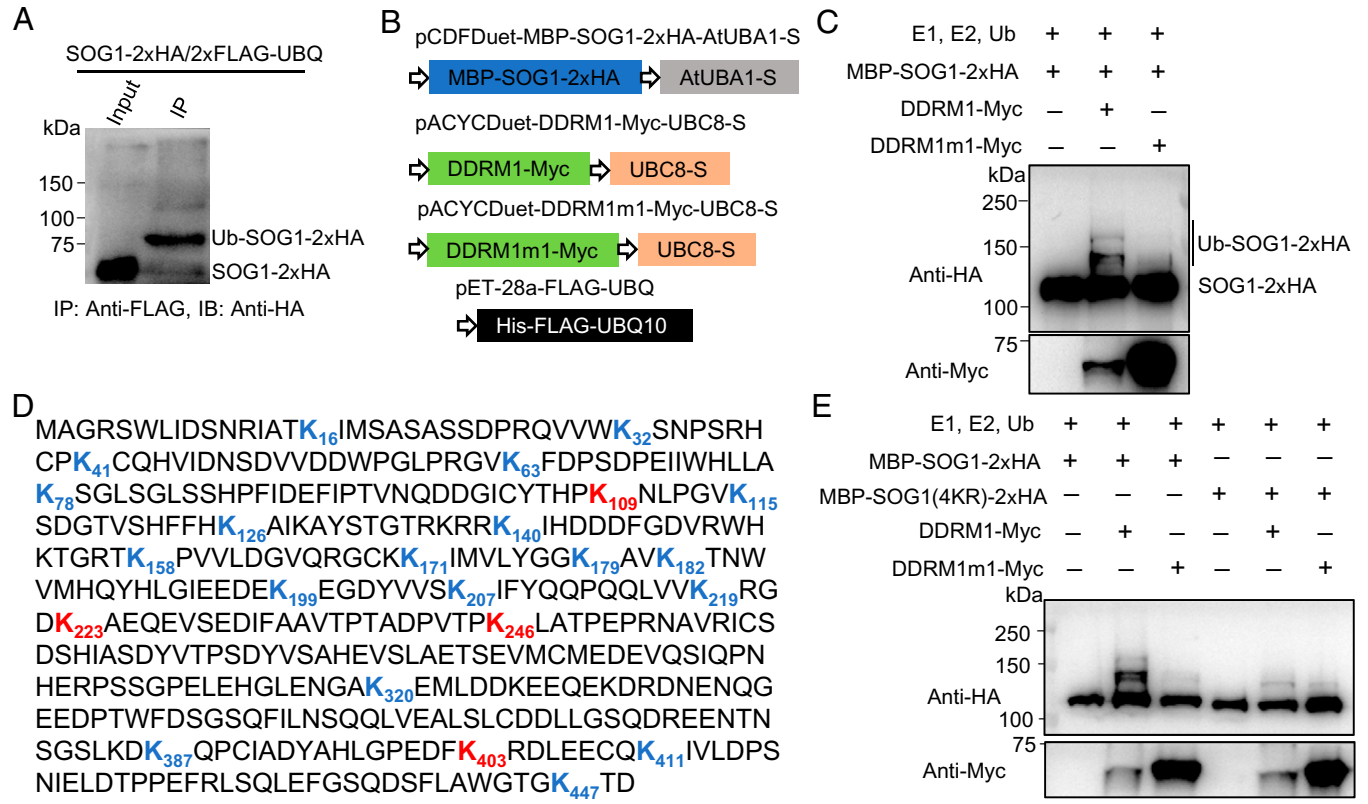

Fig. 5. DDRM1 ubiquitinates SOG1. (*A*) SOG1 fused with two tandem HA tag (SOG1-2xHA) and ubiquitin (UBQ) fused with two tandem FLAG tag (2xFLAG-UBQ) were coexpressed in *Arabidopsis* protoplasts. Total proteins were extracted and immunoprecipitated with FLAG beads. Both the input and immunoprecipitated samples were subjected to Western blotting using anti-HA antibody. (*B*) Schematic diagrams of the constructs used for the ubiquitination assays in *E. coli*. SOG1 was fused to an MBP tag at its N terminus and two tandem HA tag at its C terminus. DDRM1 or DDRMm1 was fused to a Myc tag. UBQ10 was fused with His and FLAG tags. (*C*) In vitro ubiquitination assays. The constructs in (*B*) were coexpressed in *E. coli* as indicated and the bacterial lysates were subjected to Western blotting using anti-HA or anti-Myc antibodies. E1, AtUBA1-S. E2, AtUBC8-S. Ub, FLAG-UBQ10. (*D*) The ubiquitination sites of SOG1 identified by mass spectrometry. The ubiquitinated Lys (K) residues are shown in bold, with the top four residues in red. (*E*) In vitro ubiquitination assays of SOG1(4KR), in which K109, K246, K223, and K403 are mutated to Arg (R). The assay was performed as in (*C*).

DDRM1 Is Required for HR. It was reported that SOG1 is required for HR. The HR efficiency of the *sog1-101* mutant was ~20% of that of WT (44). Since DDRM1 stabilizes SOG1, we hypothesized that DDRM1 is also required for HR. To test the HR efficiency of *ddrm1-2*, we used a previously established HR reporter system including the reporter lines (DU.GUS or IU.GUS) and the I-SceI trigger line (45). The difference between DU.GUS and IU.GUS is that the nearby donor sequence (U) is in the direct and inverted orientation, respectively. HR between the nonfunctional *GUS* and the donor sequence produces functional *GUS* gene, which results in blue sectors after GUS staining. Both the reporter lines and the I-SceI trigger line were introduced into the *ddrm1-2* mutant through genetic crossing. The HR efficiency was determined by counting the number of blue spots in the cotyledons of F1 seedlings. Compared with WT, the relative HR efficiency of *ddrm1-2* was reduced to 13.4% and 42.8% in the IU.GUS and DU.GUS system, respectively (Fig. 8 *A*–*F*). These results strongly supported that DDRM1 is required for HR.

Discussion

Numerous studies in animals revealed that ubiquitination plays important roles in DDR (20–22, 24). However, it is unclear how ubiquitination regulates plant DDR. In mammals, the RING-containing protein RNF8 is required for HR (20, 25). Although *Arabidopsis* does not contain RNF8 orthologs, it encodes more than 450 RING-containing proteins (46), most of which are not functionally studied. In this study, we identified DDRM1 as a plant-specific regulator of HR. Based on our data, we proposed a simple working model to illustrate how DDRM1 functions to promote HR (Fig. 8*G*). In the absence of DSBs, SOG1 is polyubiquitinated by an unknown E3 ligase and is subsequently degraded. Upon detection of DSBs, plants can activate DDRM1, which ubiquitinates SOG1 at multiple sites, and stabilize SOG1. The stabilized SOG1 regulates DDR including cell-cycle arrest, transcription reprogramming, DNA repair, and cell death. Since both SOG1 and DDRM1 are highly conserved in plants, it is likely that DDRM1-SOG1 represents a plant-specific module required for HR. Our study not only identified a plant-specific DDR regulator but also suggested that ubiquitination is also an important mechanism in plant DDR, significantly advancing our understanding of HR. Given that SOG1 regulates many aspects of DDR and DDRM1 regulates SOG1, it is likely that DDRM1 is involved in other aspects of DDR in addition to HR, which is worthwhile studying in the future. Furthermore, it will be very interesting to study how plants activate DDRM1.

SOG1 is considered as the plant counterpart of p53, which is regulated by various forms of posttranslational modifications including phosphorylation and ubiquitination (47–49). The ubiquitination of p53 is very important for its

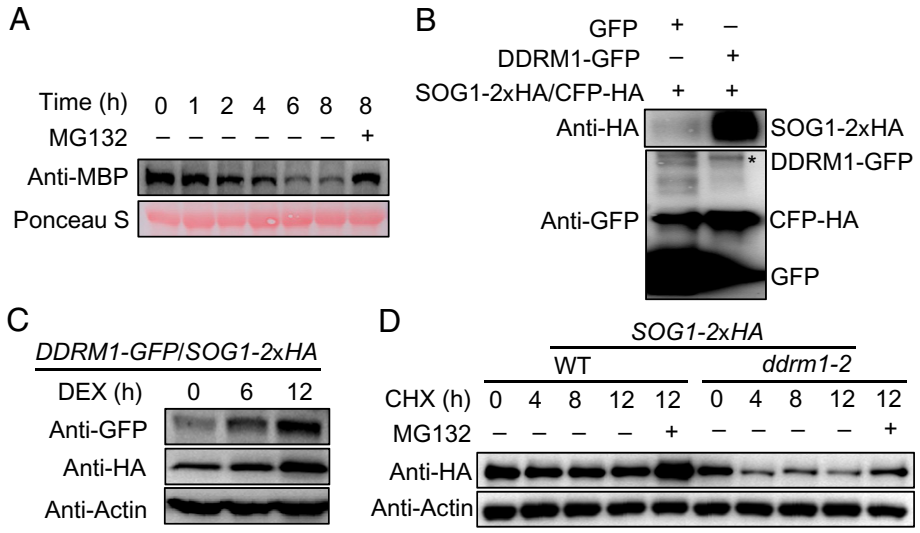

Fig. 6. DDRM1 promotes the stability of SOG1. (*A*) SOG1 is degraded through 26S proteasome. The MBP-SOG1 recombinant protein was incubated with total protein extract of 8-d-old seedlings at 25 °C for different time. The Western blotting was performed using an anti-MBP antibody. Ponceau S staining was used as a loading control. MG132, the inhibitor of 26S proteasome. (*B*) DDRM1 stabilizes SOG1 in *N. benthamiana*. SOG1-2xHA was coexpressed with GFP or DDRM1-GFP in *N. benthamiana*. The total proteins were subjected to Western blotting using anti-GFP or anti-HA antibodies. CFP-HA in the same vector of SOG1-2xHA was served as the control for transformation efficiency. (*C*) DDRM1 stabilizes SOG1 in *Arabidopsis*. *DDRM1-GFP* driven by the Dexamethasone (DEX)-inducible promoter pGVG was transformed into *35S:SOG1-2xHA/ddrm1-2*. The 8-d-old transgenic plants were treated with 25 μM DEX for different time and were subjected to Western blotting using anti-HA, anti-GFP, and anti-Actin antibodies. Actin was used as a loading control. (*D*) In vivo degradation assays. The 8-d-old transgenic plants expressing 35S:SOG1-2xHA in either WT or *ddrm1-2* were treated with 300 μM chlorhexidine (CHX) to inhibit protein synthesis for different time and were subjected to Western blotting using anti-HA and anti-Actin antibodies. MG132 (100 μM) was added to the indicated samples to inhibit protein degradation.

function and was well-studied. p53 can be either monoubiquitinated or polyubiquitinated, depending on the biological context (48). However, it is unknown whether SOG1 is regulated by ubiquitination. In this study, we demonstrated that SOG1 can be ubiquitinated by DDRM1. Based on the ubiquitination assays (Fig. 5*A*), we proposed that SOG1 is monoubiquitinated at multiple sites. Since SOG1 was degraded through 26S proteasome (Fig. 6*A*), it is likely that SOG1 is also polyubiquitinated by an unknown ubiquitin E3 ligase. Given that DDRM1 promoted the stability of SOG1, the monoubiquitination of SOG1 may inhibits its polyubiquitination. Although the detailed mechanisms require further studies, our study demonstrated that ubiquitination is an important regulatory mechanism of SOG1.

In addition to RING domain at the C terminus, both RNF8 and DDRM1 contain another protein domain at the N terminus, with forkhead-associated (FHA) domain in RNF8 and BRCT domain in DDRM1. Interestingly, both FHA and BRCT domains are phosphopeptide recognition domain (40, 50). It was reported that RNF8 binds the phosphorylated MDC1 (20). We found that DDRM1 interacts with SOG1, which could be phosphorylated by ATM, ATR, and CK2 (30, 31). It is likely that the phosphorylation of SOG1 promotes its interaction with DDRM1. In addition to SOG1, DDRM1 may bind to other phosphorylated proteins, which will be the subject of future study. Given the similarities of RNF8 and DDRM1 in structure and function, it is possible that DDRM1 may be a functional counterpart of RNF8 in plants.

Phylogenetic analysis revealed that DDRM1 is an evolutionarily ancient protein, which is identified in the first land plants, mosses, but not in the aquatic algae (Fig. 2*A*), indicating that DDRM1 is evolved to adapt to the harsher environment of land. The involvement of DDRM1 in DDR suggests that the capacity of DNA damage repair is one of the driving forces for plant evolution from aquatic to land.

Materials and Methods

Plant Materials and Growth Conditions. All *Arabidopsis thaliana* used in this study are in Columbia (Col-0) background. The TRANSPLANTA collection (N2101415) and the *ddrm1-2* (GABI_910B12) were obtained from Nottingham *Arabidopsis* Stock Centre (NASC). The *atm-2* (SALK_006953) mutant was obtained from *Arabidopsis* Biological Resource Center (ABRC). The transgenic *Arabidopsis* were generated by floral-dip method (51). Seeds were sterilized with 2% PPM (Plant Cell Technology), stratified at 4 °C in the dark for 2 d, and then plated on 1/2 Murashige and Skoog (MS) medium containing 1% sucrose and 0.3% phytagel with or without 20 nM CPT, 5 μM BLM, 75 μg/mL MMS, or 1 mM HU. The plants were grown under long-day conditions (16 h of light and 8 h of dark) at 22 °C in a growth chamber. The primers for genotyping were listed in *SI Appendix*, Table S1.

Mutant Screening. The TRANSPLANTA collection was used to screen for *ddrms*. In the primary screening, the seeds from individual lines were plated on 1/2 MS medium containing 20 nM CPT and 10 μM β-estradiol and grown vertically for 7–9 d. The plants with shorter or longer roots than WT were considered as putative *ddrms*, which were subjected for rescreening on 1/2 MS medium containing 20 nM CPT in the presence or absence of 10 μM β-estradiol. The *atm-2* mutant was used as a positive control in screening.

Vector Constructions. The vectors were constructed using digestion–ligation method, Gateway technology (Thermo Fisher Scientific), or Lighting Cloning System (Biodragon Immunotechnology). The primers used for vector construction were listed in *SI Appendix*, Table S1.

Generation of Transgenic *Arabidopsis*. The CDS of *DDRM1* or its mutants (*DDRM1m1* and *DDRM1m2*) were cloned into pFGC5941 vector at NcoI and BamHI sites to generate 35S:DDRM1, 35S:DDRM1m1, or 35S:DDRM1m2 constructs. The CDS of *SOG1* was fused with a 2xHA tag and cloned into NcoI/BamHI-digested pFGC5941 vector to obtain 35S:SOG1-2xHA construct. The *DDRM1* promoter (1,500 bp fragment upstream of the start codon) was cloned into SalI/BamHI-digested pCAM2300-H2B-YFP-GUS vector to generate pDDRM1:H2B-YFP-GUS. The CDS of *DDRM1* was cloned into pDONR207, and then introduced into pMDC43 to generate 35S:GFP-DDRM1 using gateway technology (Thermo Fisher). These vectors were transformed into *Agrobacterium tumefaciens GV3101*, which were used to transformed into *Arabidopsis* using

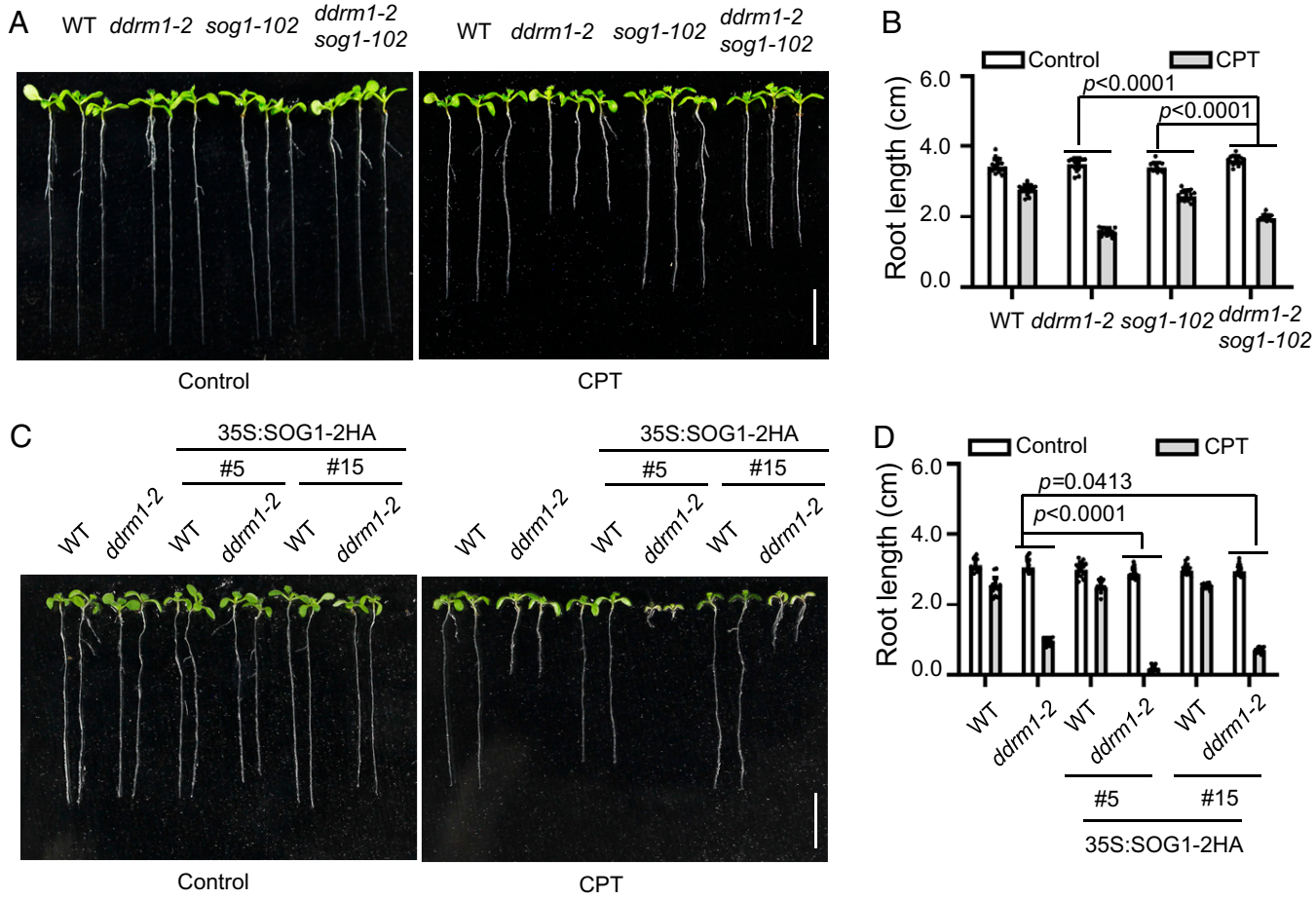

Fig. 7. SOG1 functions downstream of DDRM1. (*A*, *B*) Loss of function of SOG1 partially rescues the hypersensitivity of *ddrm1-2* to CPT. Plants were grown vertically on the control medium or the medium containing 10 nM CPT for 8 d. (*C*, *D*) Overexpressing SOG1 enhances the hypersensitivity of *ddrm1-2* to CPT. The SOG1 driven by the 35S promoter was transformed into WT and *ddrm1-2*. Two independent transgenic lines were grown vertically on the control medium or the medium containing 20 nM CPT for 8 d. The photos (*A*, *C*) and root length (*B*, *D*) of plants were shown. (Scale bars: 1 cm.) The root length was represented as means ± SD (n = 15). The statistical significance was determined using two-way ANOVA analysis.

the floral-dip method. *35S:SOG1-2xHA/WT* was crossed with *ddrm1-2* to generate *35S:SOG1-2xHA/ddrm1-2*. Homozygous T3 or F3 lines were used for further study.

Gene Expression Analysis. Total RNA was isolated using TRIpure Reagent (Aidlab). The total RNA (1 μg) was used for gDNA removal and cDNA synthesis using the HiScript II Q RT SuperMix kit (R223-01, Vazyme). The cDNA was diluted five times and was used as template for RT-PCR using 2xEs Taq MasterMix (CW0690S, CoWin Biosciences). *Ubiquitin 5* (*UBQ5*) was used as the reference gene. The primer sequences used for RT-PCR were listed in *SI Appendix*, Table S1.

Sequence Alignment and Phylogenetic Analysis of DDRM1 Orthologs. The protein sequences of DDRM1 orthologs were retrieved using the BLASTP program at the National Center for Biotechnology Information (NCBI) (https://blast.ncbi.nlm.nih.gov/Blast.cgi). The phylogenetic trees for the DDRM1 orthologs were constructed using MEGA-X (52). Protein structures were illustrated by PfamScan. The protein sequence alignment was performed using DNAMAN 7.

Subcellular Localization Assay. For subcellular localization assays, 35S:GFP-DDRM1 was transiently expressed in *N. benthamiana*. After 2 d, the GFP fluorescence was captured using confocal microscopy (TCS SP8, Leica). The root of *35S:GFP-DDRM1* transgenic seedlings was stained with propidium iodide (PI), and the PI and GFP fluorescences were captured by confocal microscopy (TCS SP8, Leica).

GUS Staining. The GUS staining assays were performed as described previously (53). Seedlings were stained overnight in X-Gluc solution (50 mM sodium phosphate pH 7.0, 50 mM EDTA pH 8.0, 0.5 mM $K_3Fe(CN)_6$, 0.5 mM $K_4Fe(CN)_6$, 0.1% Triton X-100, 1 mM X-Gluc, 20% methanol) at 37 °C. The chlorophyll was cleared out of the samples using 70% ethanol. Images of seedlings and roots were taken using an Olympus DP72 Digital Microscope Camera.

BiFC Assay. For BiFC assay, the CDS of *DDRM1* or *SOG1* were cloned into the pEarley-YN or pEarley-YC vectors using Gateway technology. The resulting vectors were transiently expressed in *N. benthamiana*. The images were captured using confocal microscopy (TCS SP8, Leica).

Split Luciferase Assay. Split luciferase assay was performed as described previously (42). The CDS of *SOG1* or *DDRM1* was cloned into pJW771 or pJW772 at KpnI and SalI sites to generate SOG1-nLUC or cLUC-DDRM1. The resulting constructs were transiently expressed in the leaves of *N. benthamiana*. After 2 d, 1 mM luciferin was sprayed to the injected leaves and the images were captured using Lumazone imaging system equipped with 2048B CCD camera (Roper).

CoIP Assay. The CDS of *SOG1* was cloned into NcoI/BamHI-digested pFGC5941-GFP vector to generate 35S:SOG1-GFP construct. The CDS of *DDRM1m1* was cloned into KpnI/SalI-digested pCambia2306 vector to obtain 35S:DDRM1m1-3xFLAG construct. *Agrobacterium* containing 35S:DDRM1m1-3xFLAG was coinfiltrated with 35S:GFP or 35S:SOG1-GFP into leaves of *N. benthamiana*. After 60 h, the collected leaves were ground in liquid nitrogen and total proteins were extracted with RIPA buffer containing 100 mM Tris-HCl pH 7.5, 150 mM NaCl, 0.5 mM EDTA, 1% Triton X-100, 1% deoxycholate, 0.1% SDS, 10% glycerol, 1 mM PMSF, 100 μM MG132 (MedChemExpress). The diluted lysate was incubated with 10 μL GFP-Trap Magnetic Beads (Chromotek) at 4 °C for 4 h. The beads were washed four times with Western and IP lysis buffer

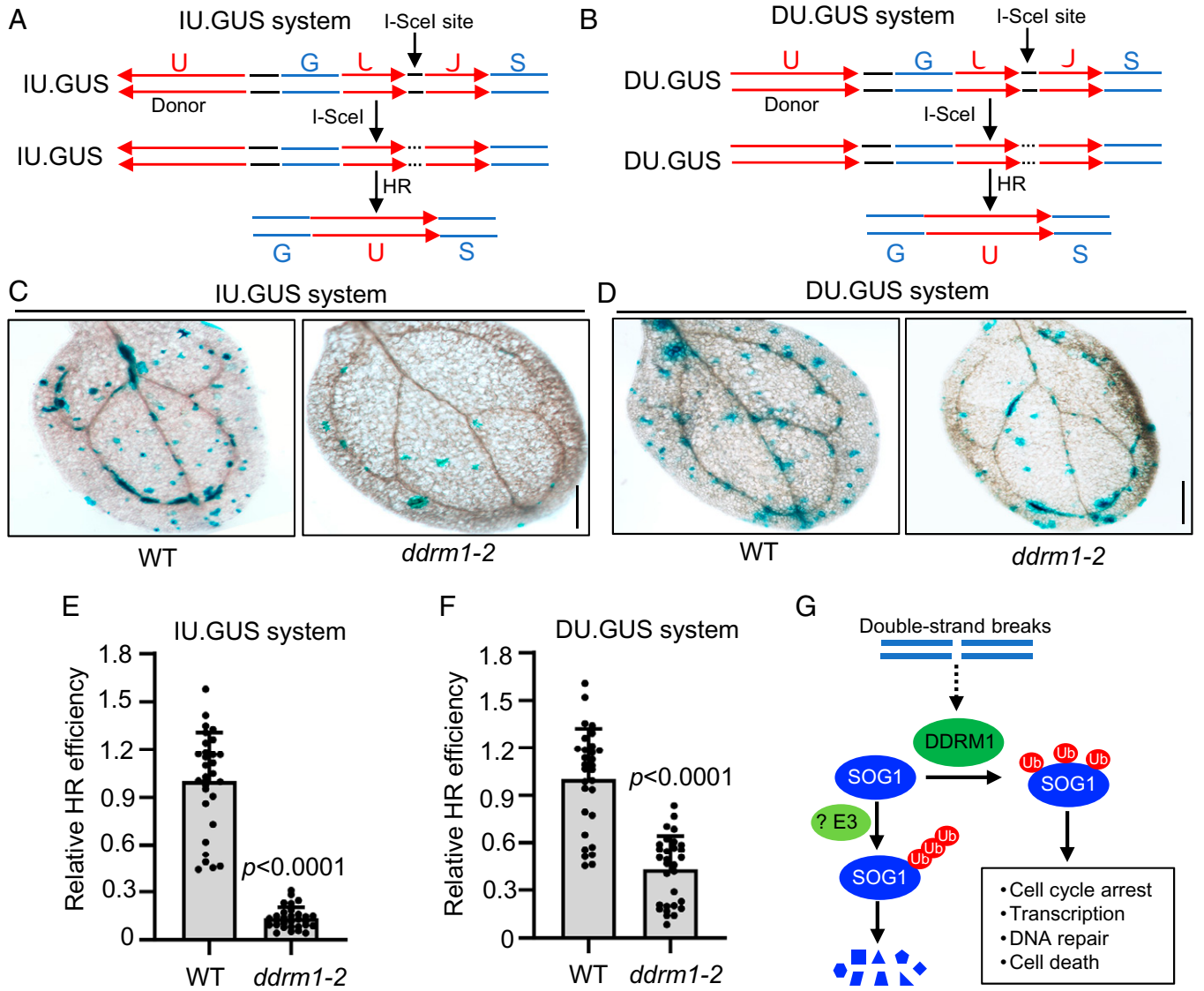

Fig. 8. DDRM1 is required for HR. (*A*, *B*) Schematic representation of HR reporter system, IU.GUS (*A*) and DU.GUS (*B*). The reporter line contains a recognition site for the restriction endonuclease I-SceI within the GUS gene as well as a nearby donor sequence (U) in direct (DU.GUS) or inverted orientation (IU.GUS). A single DSB is induced when the reporter line is crossed with the I-SceI trigger line. When the DSB is repaired through HR, the functional GUS is restored. (*C*, *D*) Representative GUS staining images of cotyledon in the IU.GUS reporter system (*C*) or DU.GUS reporter system (*D*). The reporter line and trigger line in either *ddrm1-2* or WT background were crossed and the F1 seedlings were used for scoring. (Scale bar: 0.5 mm.) (*E*, *F*) The relative HR efficiency. For each genotype, the number of blue sectors from 30 plants was scored. The data were represented as means ± SD ($n = 30$). The statistical significance was determined using Student's *t* test. (*G*) A simplified model for DDRM1-SOG1 in HR. SOG1 can be polyubiquitinated by an unknown ubiquitin E3 ligase, leading to its degradation through 26S proteome. After activation by double-strand breaks, DDRM1 ubiquitinates SOG1 at multiple sites, enhancing the stability of SOG1, which triggers DNA damage responses including cell-cycle arrest, transcription reprogramming, DNA repair, and cell death. Ub, ubiquitination.

(P0013, Beyotime) and subjected to immunoblot analysis with anti-FLAG (1:4,000, Promoter) or anti-GFP (1:4,000, Promoter).

Pull-Down Assay. The CDS of *DDRM1* was cloned into BamHI/XhoI-digested pGEX4T-3 to generate GST-DDRM1 construct. The CDS of *SOG1* was cloned into NdeI/EcoRI-digested pMAL-c5X to generate MBP-SOG1 construct. These constructs were individually transformed into *E. coli* BL21 (DE3). The recombinant proteins were induced with 0.5 mM IPTG at 20 °C for 16 h. MBP-SOG1 was purified using Amylose Resin (New England BioLabs) and was incubated with GST or GST-DDRM1 coupled with Glutathione-Sepharose Resin (CW0190, CoWin Biosciences) in the binding buffer (50 mM Tris-HCl pH 7.5, 150 mM NaCl, 1 mM PMSF, 1 mM EDTA, and 0.1% Triton X-100) at 4 °C for 2 h. After washing five times with washing buffer (50 mM Tris-HCl pH 7.5, 300 mM NaCl, 1 mM EDTA, and 0.4% Triton X-100), the bound proteins were analyzed by Western blotting using anti-GST (1:5,000, ABclonal) and anti-MBP (1:5,000, ABclonal) antibodies.

In Vivo Ubiquitination Assay. In vivo ubiquitination assay was performed as described previously (54), with slight modifications. In brief, the 35S:SOG1-2xHA and 35S:2xFLAG-UBQ vectors were coexpressed in *Arabidopsis* protoplasts. Protoplasts were incubated at room temperature for 10 h and then were treated with 20 μM MG132 for another 8 h before harvest. Total proteins were extracted with Western and IP lysis buffer (P0013, Beyotime) containing 100 μM MG132 and 1 mM PMSF. The lysate was incubated with 10 μL anti-FLAG Magnetic Beads (L-1011, Biolinkedin) at 4 °C for 4 h. The beads were washed three times with Western and IP lysis buffer and were subjected to Western blotting analysis using an anti-HA (1:2,000, ABclonal) antibody.

In Vitro Ubiquitination Assay. The in vitro ubiquitination assay was performed as described previously in *E. coli* (43). SOG1 was fused to an MBP tag at its N terminus and a hemagglutinin (2xHA) tag at its C terminus to generate pCDFDuet-MBP-SOG1-2xHA-AtUBA1-S. DDRM1 or DDRM1m1 was fused to a Myc tag at its C terminus to generate pACYCDuet-DDRM1-Myc-AtUBC8-S or pACYCDuet-DDRM1m1-Myc-AtUBC8-S. Different combinations of vectors were transformed into *E. coli* BL21 (DE3). The recombinant protein expression was induced with 0.5 mM IPTG at 20 °C for 16 h, and then the cells were incubated

at 28 °C for 12 h to allow ubiquitination, followed by incubation at 4 °C overnight. The cell lysates were subjected to Western blotting analysis using anti-HA (1:5,000, ABclonal) and anti-Myc (1:4,000, Promoter) antibodies.

Identification of Ubiquitination Sites through Mass Spectrometry. The MBP-SOG1-2xHA from the ubiquitination assay in *E. coli* was purified using Amylose Resin (New England BioLabs) and were digested on the beads with trypsin at 37 °C overnight. The resultant peptides were analyzed on an Ultimate 3000 nano UHPLC system (Thermo Fisher Scientific) coupled online to a hybrid Quadrupole-Orbitrap mass spectrometer Q Exactive HF (Thermo Fisher Scientific). The raw data were processed using "Peaks DB Search" function of Peaks Studio version 8.5 (Bioinformatics Solutions) with ubiquitination of lysine residues as a variable modification against Araport11 protein database.

Cell-Free Degradation Assay. The cell-free degradation assay was performed as described previously (55). The MBP-SOG1 recombinant protein was incubated with total proteins extracted from *Arabidopsis* seedlings using native protein extraction buffer (50 mM Tris-MES pH 8.0, 10 mM EDTA pH 8.0, 0.5 M Sucrose, 1 mM $MgCl_2$, 1 mM PMSF, and 5 mM DTT) at room temperature for different time. The MBP-SOG1 protein was detected by Western blotting using anti-MBP (1:5,000, ABclonal) antibody.

In Vivo Degradation Assay. The *35S:SOG1-2xHA/WT* and *35S:SOG1-2xHA/ddrm1-2* seedlings were treated with 300 μM CHX for different times with or without 100 μM MG132. Total proteins were extracted with RIPA lysis buffer (P0013B, Beyotime) and subjected to Western blotting analysis using anti-HA (1:2,000, ABclonal) antibody.

HR Efficiency Assay. The HR efficiency assay was performed as previously described (45). The DU.GUS and IU.GUS reporters were used. The reporter line and trigger line were crossed with the *ddrm1-2* mutant, respectively. In the F2 generation, the homozygous lines for reporter, trigger, and *ddrm1-2* were identified through genotyping. The homozygous reporter line in *ddrm1-2* was crossed with the homozygous trigger line in *ddrm1-2,* and the homozygous reporter line in WT was crossed with the homozygous trigger line in WT. The resulting F1 plants were used for GUS staining.

Statistical Analysis. Statistical tests were performed using GraphPad Prism 8.

Data Availability. All study data are included in the article and/or supporting information.

ACKNOWLEDGMENTS. We are grateful to Dr. Dongping Lu for providing the vectors for in vitro ubiquitination assays and Dr. Yijun Qi for providing the seeds of HR reporter systems. This work was supported by the National Natural Science Foundation of China (31970311, 31800216, and 32000372); Thousand Talents Plan of China-Young Professionals Grant; Huazhong Agricultural University Scientific & Technological Self-innovation Foundation (2014RC004); and Long Yun program and Bai Chuan program of College of Life Science and Technology, Huazhong Agricultural University.

1. A. Maréchal, L. Zou, DNA damage sensing by the ATM and ATR kinases. *Cold Spring Harb. Perspect. Biol.* **5**, a012716 (2013).
2. H. Keskin *et al.*, Transcript-RNA-templated DNA recombination and repair. *Nature* **515**, 436–439 (2014).
3. J. A. Marteijn, H. Lans, W. Vermeulen, J. H. Hoeijmakers, Understanding nucleotide excision repair and its roles in cancer and ageing. *Nat. Rev. Mol. Cell Biol.* **15**, 465–481 (2014).
4. C. J. Lord, A. Ashworth, The DNA damage response and cancer therapy. *Nature* **481**, 287–294 (2012).
5. A. B. Britt, DNA damage and repair in plants. *Annu. Rev. Plant Physiol. Plant Mol. Biol.* **47**, 75–100 (1996).
6. D. Yi *et al.*, The *Arabidopsis* SIAMESE-RELATED cyclin-dependent kinase inhibitors SMR5 and SMR7 regulate the DNA damage checkpoint in response to reactive oxygen species. *Plant Cell* **26**, 296–309 (2014).
7. K. O. Yoshiyama, K. Sakaguchi, S. Kimura, DNA damage response in plants: Conserved and variable response compared to animals. *Biology (Basel)* **2**, 1338–1356 (2013).
8. Z. Hu, T. Cools, L. De Veylder, Mechanisms used by plants to cope with DNA damage. *Annu. Rev. Plant Biol.* **67**, 439–462 (2016).
9. V. Manova, D. Gruszka, DNA damage and repair in plants – From models to crops. *Front. Plant Sci.* **6**, 885 (2015).
10. M. U. Nisa, Y. Huang, M. Benhamed, C. Raynaud, The plant DNA damage response: Signaling pathways leading to growth inhibition and putative role in response to stress conditions. *Front. Plant Sci.* **10**, 653 (2019).
11. M. R. Lieber, The mechanism of double-strand DNA break repair by the nonhomologous DNA end-joining pathway. *Annu. Rev. Biochem.* **79**, 181–211 (2010).
12. W. D. Heyer, K. T. Ehmsen, J. Liu, Regulation of homologous recombination in eukaryotes. *Annu. Rev. Genet.* **44**, 113–139 (2010).
13. E. Sonoda, H. Hochegger, A. Saberi, Y. Taniguchi, S. Takeda, Differential usage of non-homologous end-joining and homologous recombination in double strand break repair. *DNA Repair (Amst.)* **5**, 1021–1029 (2006).
14. M. D. Canny *et al.*, Inhibition of 53BP1 favors homology-dependent DNA repair and increases CRISPR-Cas9 genome-editing efficiency. *Nat. Biotechnol.* **36**, 95–102 (2018).
15. D. Miki, W. Zhang, W. Zeng, Z. Feng, J. K. Zhu, CRISPR/Cas9-mediated gene targeting in *Arabidopsis* using sequential transformation. *Nat. Commun.* **9**, 1967 (2018).
16. F. Fauser *et al.*, In planta gene targeting. *Proc. Natl. Acad. Sci. U.S.A.* **109**, 7535–7540 (2012).
17. T. Uziel *et al.*, Requirement of the MRN complex for ATM activation by DNA damage. *EMBO J.* **22**, 5612–5621 (2003).
18. J. Lukas, C. Lukas, J. Bartek, More than just a focus: The chromatin response to DNA damage and its role in genome integrity maintenance. *Nat. Cell Biol.* **13**, 1161–1169 (2011).
19. M. Stucki *et al.*, MDC1 directly binds phosphorylated histone H2AX to regulate cellular responses to DNA double-strand breaks. *Cell* **123**, 1213–1226 (2005).
20. N. K. Kolas *et al.*, Orchestration of the DNA-damage response by the RNF8 ubiquitin ligase. *Science* **318**, 1637–1640 (2007).
21. F. Mattiroli *et al.*, RNF168 ubiquitinates K13-15 on H2A/H2AX to drive DNA damage signaling. *Cell* **150**, 1182–1195 (2012).
22. T. Thorslund *et al.*, Histone H1 couples initiation and amplification of ubiquitin signalling after DNA damage. *Nature* **527**, 389–393 (2015).
23. B. Wang, S. J. Elledge, Ubc13/Rnf8 ubiquitin ligases control foci formation of the Rap80/Abraxas/Brca1/Brcc36 complex in response to DNA damage. *Proc. Natl. Acad. Sci. U.S.A.* **104**, 20759–20763 (2007).
24. G. S. Stewart *et al.*, The RIDDLE syndrome protein mediates a ubiquitin-dependent signaling cascade at sites of DNA damage. *Cell* **136**, 420–434 (2009).
25. P. Schwertman, S. Bekker-Jensen, N. Mailand, Regulation of DNA double-strand break repair by ubiquitin and ubiquitin-like modifiers. *Nat. Rev. Mol. Cell Biol.* **17**, 379–394 (2016).
26. R. Prakash, Y. Zhang, W. Feng, M. Jasin, Homologous recombination and human health: The roles of BRCA1, BRCA2, and associated proteins. *Cold Spring Harb. Perspect. Biol.* **7**, a016600 (2015).
27. K. Yoshiyama, P. A. Conklin, N. D. Huefner, A. B. Britt, Suppressor of gamma response 1 (SOG1) encodes a putative transcription factor governing multiple responses to DNA damage. *Proc. Natl. Acad. Sci. U.S.A.* **106**, 12843–12848 (2009).
28. K. O. Yoshiyama, S. Kimura, H. Maki, A. B. Britt, M. Umeda, The role of SOG1, a plant-specific transcriptional regulator, in the DNA damage response. *Plant Signal. Behav.* **9**, e28889 (2014).
29. N. Ogita *et al.*, Identifying the target genes of SUPPRESSOR OF GAMMA RESPONSE 1, a master transcription factor controlling DNA damage response in *Arabidopsis*. *Plant J.* **94**, 439–453 (2018).
30. K. O. Yoshiyama, K. Kaminoyama, T. Sakamoto, S. Kimura, Increased phosphorylation of Ser-Gln sites on SUPPRESSOR OF GAMMA RESPONSE1 strengthens the DNA damage response in *Arabidopsis thaliana*. *Plant Cell* **29**, 3255–3268 (2017).
31. P. Wei *et al.*, *Arabidopsis* casein kinase 2 triggers stem cell exhaustion under Al toxicity and phosphate deficiency through activating the DNA damage response pathway. *Plant Cell* **33**, 1361–1380 (2021).
32. Y. Pommier, Topoisomerase I inhibitors: Camptothecins and beyond. *Nat. Rev. Cancer* **6**, 789–802 (2006).
33. T. Takahashi, S. Matsuhara, M. Abe, Y. Komeda, Disruption of a DNA topoisomerase I gene affects morphogenesis in *Arabidopsis*. *Plant Cell* **14**, 2085–2093 (2002).
34. C. H. Liu *et al.*, Repair of DNA damage induced by the cytidine analog zebularine requires ATR and ATM in *Arabidopsis*. *Plant Cell* **27**, 1788–1800 (2015).
35. A. Coego *et al.*; TRANSPLANTA Consortium, The TRANSPLANTA collection of *Arabidopsis* lines: A resource for functional analysis of transcription factors based on their conditional overexpression. *Plant J.* **77**, 944–953 (2014).
36. Y. G. Liu, Y. Chen, High-efficiency thermal asymmetric interlaced PCR for amplification of unknown flanking sequences. *Biotechniques* **43**, 649–650, 652, 654 passim (2007).
37. N. Elrouby, M. V. Bonequi, A. Porri, G. Coupland, Identification of *Arabidopsis* SUMO-interacting proteins that regulate chromatin activity and developmental transitions. *Proc. Natl. Acad. Sci. U.S.A.* **110**, 19956–19961 (2013).
38. K. Riha, J. M. Watson, J. Parkey, D. E. Shippen, Telomere length deregulation and enhanced sensitivity to genotoxic stress in *Arabidopsis* mutants deficient in Ku70. *EMBO J.* **21**, 2819–2826 (2002).
39. A. K. Weimer *et al.*, The plant-specific CDKB1-CYCB1 complex mediates homologous recombination repair in *Arabidopsis*. *EMBO J.* **35**, 2068–2086 (2016).
40. X. Yu, C. C. Chini, M. He, G. Mer, J. Chen, The BRCT domain is a phospho-protein binding domain. *Science* **302**, 639–642 (2003).
41. R. J. Deshaies, C. A. Joazeiro, RING domain E3 ubiquitin ligases. *Annu. Rev. Biochem.* **78**, 399–434 (2009).
42. H. Chen *et al.*, Firefly luciferase complementation imaging assay for protein-protein interactions in plants. *Plant Physiol.* **146**, 368–376 (2008).
43. Y. Han *et al.*, Reconstitution of the plant ubiquitination cascade in bacteria using a synthetic biology approach. *Plant J.* **91**, 766–776 (2017).
44. N. Takahashi *et al.*, A regulatory module controlling stress-induced cell cycle arrest in *Arabidopsis*. *eLife* **8**, e43944 (2019).
45. N. Roth *et al.*, The requirement for recombination factors differs considerably between different pathways of homologous double-strand break repair in somatic plant cells. *Plant J.* **72**, 781–790 (2012).
46. S. L. Stone *et al.*, Functional analysis of the RING-type ubiquitin ligase family of *Arabidopsis*. *Plant Physiol.* **137**, 13–30 (2005).
47. W. T. Steegenga, A. J. van der Eb, A. G. Jochemsen, How phosphorylation regulates the activity of p53. *J. Mol. Biol.* **263**, 103–113 (1996).
48. S. Bang, S. Kaur, M. Kurokawa, Regulation of the p53 family proteins by the ubiquitin proteasomal pathway. *Int. J. Mol. Sci.* **21**, 261 (2019).
49. A. J. Levine, p53: 800 million years of evolution and 40 years of discovery. *Nat. Rev. Cancer* **20**, 471–480 (2020).

50. K. Hofmann, P. Bucher, The FHA domain: A putative nuclear signalling domain found in protein kinases and transcription factors. *Trends Biochem. Sci.* **20**, 347–349 (1995).
51. S. J. Clough, A. F. Bent, Floral dip: A simplified method for *Agrobacterium*-mediated transformation of *Arabidopsis thaliana*. *Plant J.* **16**, 735–743 (1998).
52. S. Kumar, G. Stecher, M. Li, C. Knyaz, K. Tamura, MEGA X: Molecular evolutionary genetics analysis across computing platforms. *Mol. Biol. Evol.* **35**, 1547–1549 (2018).
53. G. Luo, H. Gu, J. Liu, L. J. Qu, Four closely-related RING-type E3 ligases, APD1-4, are involved in pollen mitosis II regulation in *Arabidopsis*. *J. Integr. Plant Biol.* **54**, 814–827 (2012).
54. X. Ma *et al.*, Ligand-induced monoubiquitination of BIK1 regulates plant immunity. *Nature* **581**, 199–203 (2020).
55. H. Zhang *et al.*, The RING finger ubiquitin E3 ligase SDIR1 targets SDIR1-INTERACTING PROTEIN1 for degradation to modulate the salt stress response and ABA signaling in *Arabidopsis*. *Plant Cell* **27**, 214–227 (2015).